

# Scanning Electron Microscopy

---

Volume 3  
Number 1 *3rd Pfefferkorn Conference*

Article 2


---

1984

## Magnetic Electron Lenses II

T. Mulvey  
*The University of Aston in Birmingham*

Follow this and additional works at: <https://digitalcommons.usu.edu/electron>

 Part of the [Biology Commons](#)

---

### Recommended Citation

Mulvey, T. (1984) "Magnetic Electron Lenses II," *Scanning Electron Microscopy*. Vol. 3 : No. 1 , Article 2.  
Available at: <https://digitalcommons.usu.edu/electron/vol3/iss1/2>

This Article is brought to you for free and open access by the Western Dairy Center at DigitalCommons@USU. It has been accepted for inclusion in Scanning Electron Microscopy by an authorized administrator of DigitalCommons@USU. For more information, please contact [digitalcommons@usu.edu](mailto:digitalcommons@usu.edu).



MAGNETIC ELECTRON LENSES II

T. Mulvey

Department of Mathematics and Physics  
The University of Aston in Birmingham  
Birmingham B4 7ET (UK)  
Phone No. 021-359 3611

Abstract

Conventional magnetic electron lenses have evolved to their present highly developed state under the pressure of meeting the exacting requirements of high resolution electron microscopy. More recently, however, the desire to extract quantitative analytical information from the specimen has led to significant changes in the design of electron optical systems. The introduction of efficient lanthanum hexaboride cathodes and high beam current field-emission sources has strengthened this tendency. In addition, more complex lens systems than previously envisaged are now possible since microprocessors can be employed to assist in the rapid and reliable readjustment of the lens system, including the extensive alignment procedures. The use of high current density, e.g. superconducting coils, is also paving the way for new lens configurations. Furthermore, the increasing demands placed on the lens systems in electron beam lithography are bound to bring benefits to electron optical systems in general.

KEYWORDS: Magnetic Lens, Finite Element Program, Spherical Aberration, Image Distortion, Mini-lenses, Projector System, De-scan Coils, Rotation-free Lens.

Introduction

Last year we celebrated the fiftieth anniversary of high resolution electron microscopy. In November 1933 Ernst Ruska achieved a resolution better than that of the optical microscope with the aid of a new kind of magnetic electron lens - the iron shrouded polepiece lens - which he and von Borries<sup>22</sup> had patented in 1932 and which was to be decisive for the future progress of all forms of electron optical equipment. There is no consensus as to who is the inventor of the magnetic electron lens or for that matter the electron microscope, but there is, however, general agreement that iron-shrouded magnetic electron lenses sprang almost accidentally from technology rather than from science. The researches of Gabor<sup>8</sup> into the measurement of fast surges on high voltage transmission lines at the Institut für Hochspannungstechnik in 1924-6 gave birth to a crude form of what was later recognised as an iron-shrouded magnetic electron lens, the forerunner of our modern high resolution magnetic lens, the essential element in a high resolution electron microscope as well as in many other forms of electron optical instruments. Gabor's chief inspiration was to dispense with the conventional concentrating coil of the high voltage oscillograph and to replace it with a short coil encased in an iron shroud except over the axial region. His chief reason for doing so was to contain the magnetic field as far as possible within the confines of the lens itself. The main idea was to prevent any stray magnetic field from adversely affecting the operation of the cold cathode source and that of the deflecting plates used to scan the electron beam. Unwittingly he had stumbled across a way of making an efficient focussing element that worked in an entirely different way from that of the long solenoid. However, since he could not give an adequate explanation of the focussing action he is not generally considered to be the inventor of the magnetic electron lens.

The correct explanation of how such a short coil focusses the electron beam was provided later in that year by Busch<sup>5</sup> who thus became the founding father of electron optics. However, Busch found that he could not get satisfactory agreement between his theory and experimental

results that he had obtained previously on a short coil. The problem of resolving the discrepancies between experimentally measured focal properties of magnetic electron lenses and the theory calculated by Busch was resolved by Knoll and Ruska<sup>10</sup>, who in 1931 succeeded in constructing a crude electron microscope with a magnification of some 12 times using two iron free solenoids. The invention of the polepiece lens by Ruska and von Borries<sup>22</sup> was based on the idea of using iron polepieces to confine the field in a narrow gap thereby creating very high axial flux densities. Taken to its logical conclusion this led Riecke and Ruska<sup>17</sup> in 1966 to the idea of the high resolution condenser-objective lens in which the specimen is placed at the centre of the magnetic field distribution whose half-width is as small as possible and whose axial field strength is as high as possible. This lens is now widely used both in high resolution TEMs and STEMs. This lens has excellent performance but is not easy to manufacture, align, or to operate. There are also difficulties, because of the narrow objective polepiece bores and gap, in extracting x-rays, Auger electrons and other emissions from the sample.

It seems therefore that classical magnetic electron lenses and the associated electron optical systems have, after a period of fifty years of development, reached the peak of their performance. However, the demands on electron optical systems and on the lenses themselves, far from being satisfied, are becoming more pressing. This is largely due to the widespread use of electron optical instruments for analytical purposes where a great deal of information has to be extracted from the sample and the different devices such as Auger spectrometers, energy loss and x-ray spectrometers, have to be interfaced to the electron optical column. Furthermore, it is desirable that the electron optical system can be housed in a normal laboratory. Conventional lenses and columns have the grave disadvantage of occupying an enormous volume of space. High voltage microscopes are even more demanding on space and weight. This is not the only disadvantage. The large size of each lens unit restricts severely the number of lenses in the column and also their optimum placing. In the early days this was not a serious disadvantage because for manual operation it is more convenient to have as few lenses as possible. However, this does mean many electron optical compromises when the mode of operation of the instrument is changed and the same lens has to perform an incompatible number of roles. The operational difficulties of aligning and setting a multi-lens system can be largely overcome by microprocessor or computer-controlled procedures where each lens is interfaced to a central computer which stores the necessary alignment data. This paper considers some of the steps that have already been taken at the research and development level to implement the changeover to multi-lens columns of modest size and of enhanced electron optical performance.

#### Electron sources

Thermionic cathodes using tungsten filaments have held sway for approximately fifty years although in most commercial instruments they are

still in a comparatively crude state of development. The chief advantage is that the crude hairpin cathode is comparatively cheap, non-critical in alignment and tolerant of poor vacuum. Much better performance could in fact be obtained from carefully aligned pointed cathodes of oriented crystal material. For a STEM instrument a field emission cathode is essential for high resolution work but unfortunately such cathodes cannot usually produce sufficient current for analytical work with probes in the range of hundreds of nanometres. In any case a field emission system demands a superb vacuum ( $10^{-11}$  mbar) and this reduces the speed of changing specimens. Lanthanum hexaboride cathodes represent a good compromise for TEM and STEM systems. Ideally the vacuum should be just as good as for field emission systems and the temperature of the emitting crystal should be controlled by specially designed electronic circuitry. With a suitably designed LaB<sub>6</sub> cathode, it should be possible to obtain an order of magnitude improvement in source brightness compared with that of a tungsten filament. The improvement of brightness is an overriding consideration in electron optical systems since probe currents and/or exposure times will increase by the same proportion. Alternatively, for a given probe current or exposure time, the design limitations of the lenses can be correspondingly relaxed making it easier to carry out analysis more conveniently on a specimen. From an electron optical point of view, field emission guns can be improved by placing a magnetic lens in the vicinity of the emitting tip. In a field emitting gun the effective size of the cathode is of the order of nanometres. The electron beam is therefore sensitive to the effect of spherical aberration. This can be minimised by placing a suitable magnetic electron lens in the vicinity of the tip. This is easier said than done since this is a critical region for the high vacuum and also the tip is usually at a high negative potential. Nevertheless Troyon and Laberrigie<sup>20</sup> succeeded in placing a miniature magnetic electron lens just below the tip, as shown in Fig. 1. The technical difficulties associated with this construction have now been overcome and the source is now in commercial production. Another method proposed by Smith and Swann<sup>18</sup> is to immerse the emitting tip in the field of a single polepiece electron lens placed in such a way that the field strength is a maximum in the vicinity of the emitting tip, falling off gradually in the direction of the emitted electron beam. Such a lens has low spherical aberration in this configuration. There are of course practical difficulties with this arrangement. Although very promising from a theoretical point of view, it has not yet found its way into production. An interesting compromise however, between the approaches of Troyon and Laberrigie and of Smith and Swann, is shown in Fig. 2. The design is due to Venables and Archer<sup>21</sup> in which a single-polepiece lens of fairly large bore size is placed in the vicinity of the extraction electrode of the field emitting source; the shape of the axial magnetic field is not ideal, but the design is compatible with high vacuum operation and is comparatively simple to

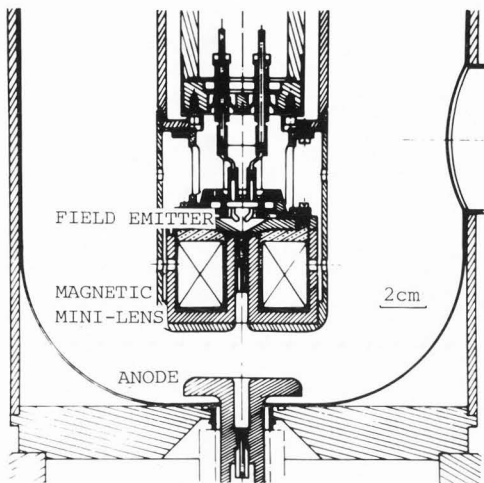


Fig. 1. Field emission electron gun (Troyon and Laberrigue 1977) with emitting tip immersed in the magnetic field of a double-polepiece mini-lens. Courtesy of the authors.

implement on existing field emission guns. Such a gun is capable of producing an appreciably greater current than is possible in the absence of the magnetic field. Furthermore, by concentrating most of the electron beam into the axial region, secondary benefits arise due to the minimisation of collisions of beam electrons with exposed metal surfaces. There is of course a limit to the improvement of the performance that can be expected merely by the use of magnetic field concentration of this kind, since with large currents, coulomb and other interactions may lead to a larger chromatic spread in the beam. Nevertheless it seems that if the vacuum is sufficiently good and the tip radius can be carefully controlled, a field emission gun with a suitably designed magnetic electron lens can give an appreciably greater beam current than is now possible with conventional field emission guns.

#### Calculation of magnetic electron lenses

The exacting specifications of magnetic electron lenses preclude the possibility of determining the final design purely by previous experience or even by a purely experimental investigation in which modifications are carried out to a well-known design until the required performance is obtained. Such procedures are time consuming and do not necessarily converge on the required solution. Fortunately great progress has been made in the last few years in numerical methods of determining lens properties and in the general area of computer-aided design. The starting point of such an investigation is the determination of the magnetic flux density distribution in the lens and especially on the lens axis. The designer must of course supply details of the structure he wishes to analyse as a basis for further refinement. Two main methods are available for determining the magnetic field distribution of a given structure. These are the finite difference method and the finite element method. The latter method is the most popular and suitable programs are generally available.

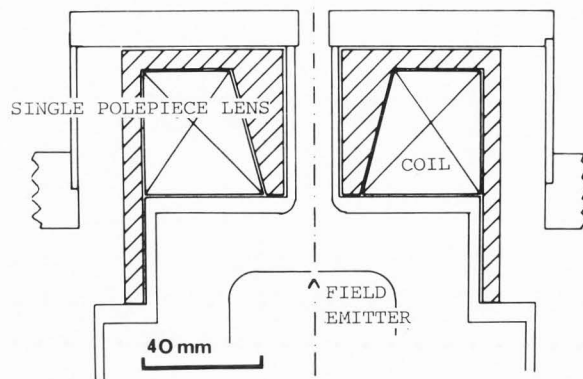


Fig. 2. Field emission electron gun (Venables and Archer 1980) with emitting tip immersed in the field of a single-polepiece lens to reduce aberrations and increase total beam current. Courtesy of J A Venables.

The finite element method is also preferred because its principle of operation, namely to minimise the energy in the magnetic structure, has perhaps an appeal on physical grounds especially where boundary problems arise, e.g. between iron and vacuum, between iron and copper, etc. Two forms of the finite element method are available: the differential form largely introduced into electron optics by Munro<sup>15</sup> in which the whole of the magnetic field distribution is divided up into finite elements and the vector potential associated with each element is determined by solving a large matrix. Boundary conditions are automatically taken into consideration and need no special attention from the program user. This means that "open" magnetic structures, whose fields extend in principle to infinity, call for very large matrices and hence very large computers if errors are to be avoided. On the other hand, the integral form of finite element method, associated in the UK with Trowbridge<sup>19</sup> and colleagues at the Rutherford-Appleton Laboratory, Harwell, follows a different approach. Here, only the coil and the magnetic circuit itself are divided into finite elements. This completely avoids the difficulty of having to divide the whole of space into finite elements. Instead, the field at any point in the magnetic circuit can be thought of as consisting of two components, one due to the coil (which can be readily calculated by the Biot-Savart law) and the other component due to the magnetisation of the iron. This magnetisation of the iron arises from the field in the iron due to the coil. The total field therefore is the sum of these two components. The iron does not itself contribute any ampere turns to the circuit, but simply modifies the flux density distribution produced by the coil. This is a valuable concept and can often be applied to check results obtained by the differential form of the finite element method. However, the price to be paid by the apparent simplicity of the integral form of the method, is that the essential information is concentrated into the small volume of the iron circuit rather

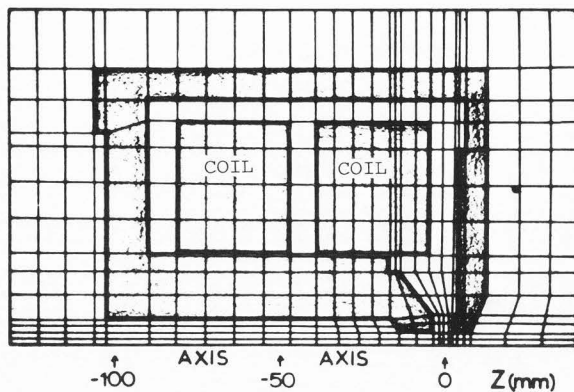


Fig. 3. Example of an early mesh layout for determining the magnetic flux distribution of a conventional magnetic objective lens. Courtesy of E Munro.

than being spread through space. This results in a very dense matrix to be inverted, with the possibility of strongly localised errors. There is therefore no saving in computer store required and so far a critical comparison has not been made of the two methods which, in the opinion of the author, should be regarded as complementary rather than competitive. Fig. 3 shows the application of Munro's programme to the determination of the field distribution in a typical conventional lens. The outer shell of the lens is unbroken except for a small air gap. This means that the external field is very small and the condition that the vector potential  $A = 0$  immediately outside the lens is satisfied. Note that whereas the lens action takes place in a volume of only a few cubic millimetres, the coil itself occupies the bulk of the space around the lens thereby restricting the possibility of placing other lenses near to the first one. The reason for this is that in the past electronic circuits were not capable of supplying large currents or large amounts of power so that the current density in the coil was low, cooling was inefficient and therefore the coil was bulky. In lenses in which one polepiece has a wide bore or in the limiting case of a single polepiece lens, as illustrated in Fig. 4, serious difficulties arise in the differential version of the finite element program. Fig. 4 shows a typical single polepiece lens with a small localised coil. Since the field from this lens extends a considerable distance away from the polepiece it is necessary to place the boundary of the area to be discretized as far away as possible. Otherwise, the boundary will appear to absorb a considerable fraction of the lens excitation. The physical explanation for this is that a surface at which the vector potential  $A = 0$  has a vanishingly small permeability, and thus acts as a super-conducting screen. If this screen is placed too near the magnetic structure it will not only remove ampere-turns from the system but will considerably distort the field distribution. This may not seriously affect the calculated focal lengths and chromatic aberration, but will almost certainly introduce serious errors into the calculation of spherical aberration. In a

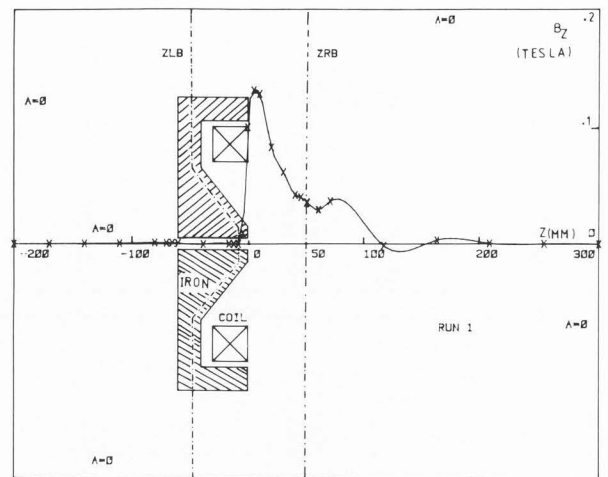


Fig. 4. Axial field distribution  $B_z$  of a single-polepiece lens by the standard finite element method with 19 (radial)  $\times$  29 (axial) element network. Spline-fitted curve through calculated points. ZLB and ZRB (dotted lines) are chosen as intermediate boundaries for subsequent refinement of the calculation<sup>13</sup>.

computer with a limited core store and hence a limited number of elements available in the axial and radial directions, further troubles will arise if the limited number of mesh points are spaced too widely. Although it is true that such effects as loss of ampere-turns and irregularities in the calculated field distribution can be minimised as the number of mesh points is increased, the errors cannot in fact be reduced to negligible proportions; furthermore each problem requires separate consideration. For computer-aided design, especially in the initial stages, great accuracy is not required provided that the resulting field distributions are smooth. What is needed most is speed of operation and the ability to interact directly with the computer. The finalised design can of course be computed in greater detail offline. By attention to detail and the introduction of some diagnostic checks, the differential finite element method can be made vastly superior to any other method for calculating electron lenses. It is also possible to carry out quite complicated calculations on a quite modest computer. Thus the field distribution in Fig. 4 was carried out on a Commodore PET Microcomputer making full use of the disk store. The axial field distribution shown in Fig. 4 is fairly smooth near the polepiece where the mesh points are fairly closely spaced and exhibits large discrete errors in the far field where fewer mesh points are available. A simple method of overcoming these defects is shown in Fig. 5. Here the previous boundary on which  $A=0$  (now shown by the dotted boundary) is replaced by another boundary (shown by the solid line) placed much closer to the lens. The vector potentials along this boundary are known from the first calculation and these are inserted on the left-hand and right-hand side respectively in Fig. 5. The calculation is re-run using the whole of the computing power within this much smaller boundary.

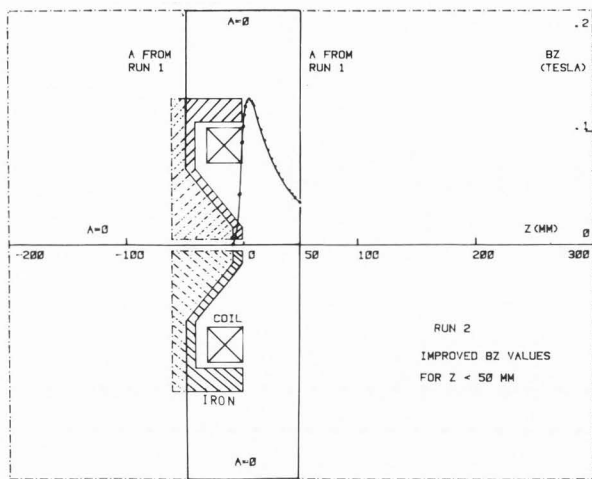


Fig. 5. Improved  $B_z$  values using  $19 \times 29$  network inside the intermediate boundary of Fig. 4.

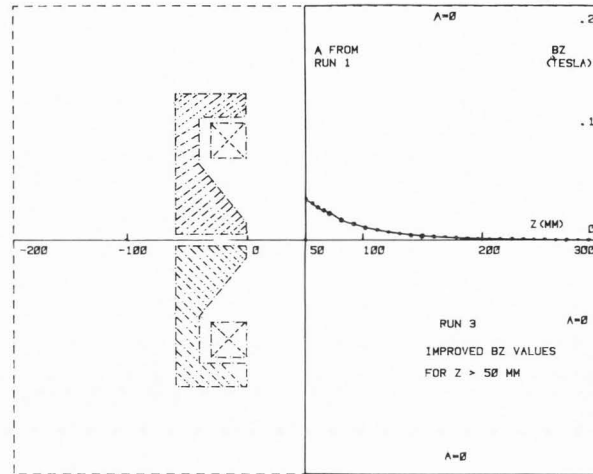


Fig. 6. Improved  $B_z$  values using  $19 \times 29$  network outside the chosen boundary of Fig. 4.

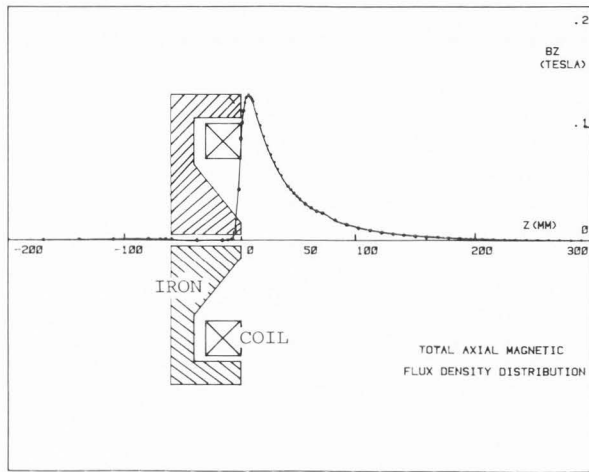


Fig. 7. Finally improved total axial field distribution of single-polepiece lens by the selected intermediate boundary method. Effective network  $19 \times 58$  (Mulvey and Nasr 1981).

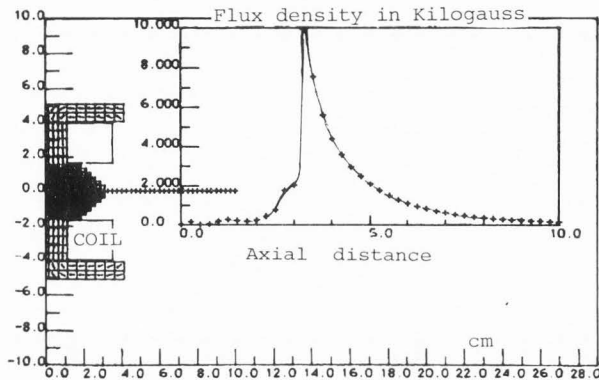


Fig. 8. Axial field distribution of single-polepiece lens calculated by the GFUN magnet design program of the Rutherford-Appleton Laboratory (courtesy of CW Trowbridge). Direction of magnetisation in iron circuit indicated by arrows. Boundary of coil also shown.

The resulting field distribution is clearly much smoother and the peak has slightly increased. The whole field can now be improved by transferring all the computer power to the right-hand side of the field as shown in Fig. 6. Here the left-hand boundary of the field, shown as a solid line, is set to the correct vector potential as found from Fig. 5 and the calculation repeated. The result is a smooth curve, as shown in Fig. 6.

Finally the total axial field distribution is shown in Figure 7. The effective network has therefore been increased to  $19 \times 58$  without increase in core store.

In this method the effective core store of the computer is increased at the expense of time. Its chief advantage is that it produces a reliably smooth field with minimal computer resources. The method is in fact analogous to that used in electrolytic tank solutions of Laplace's equation in which the potential field is first obtained

over a big area from a small model in order to determine the potentials on a much more localised boundary. The calculation is then repeated using a larger model surrounded by a more local boundary at which the potentials have been determined. It can be seen from Fig. 6 that the problem has been divided into two parts. In the first region the coil windings and associated magnetic circuit are completely contained. In the second calculation the field is determined in a region where there are no iron elements or exciting windings. A more recent and elegant method is that of Lencová and Lenc<sup>12</sup> who use a mathematical approach to determine the vector potential on the intermediate boundary between the two regions.

#### The Integral Method

Fig. 8 shows by contrast the calculation of the axial field distribution of a single pole lens by the G-FUN magnet design program<sup>19</sup> of the Rutherford-Appleton Laboratory. The iron circuit is divided into finite elements; arrows indicate the direction of magnetisation in each element.

Since the current density in the coil is assumed constant, it is only necessary to include the outline of the coil. No artificial boundary is imposed and the field at any point in space may be calculated directly. In particular, the field distribution outside the lens is perfectly smooth as would be expected since this space is not discretized. Within the polepiece region itself care has to be taken with the arrangement of the finite elements especially where the field is changing very rapidly as, for example, the sharp rise at the pole face. Fig. 9 shows a refinement of this area. These results emphasise the complementarity of the two methods. The differential method is at its weakest near the artificially imposed boundary; in addition, the smoothness of the field is liable to exhibit kinks and discontinuities even in regions remote from the exciting coil and the iron circuit because of the discretization of the whole of space. The method also tends to create errors concerning lens excitation since the area under the axial field distribution curve invariably differs from that calculated from the known lens excitation. This error usually manifests itself in an apparent loss in ampere-turns but sometimes the error can be positive indicating an apparent gain in ampere-turns. This cannot happen in the integral method but some discontinuities in the field distribution may be expected in the region occupied by the iron circuit.

#### The Differential-Integral Method<sup>13</sup>

The foregoing discussion suggests that the differential method can be considerably improved at the expense of only a trivial increase in computing time, as illustrated in Fig. 10. Here the axial flux density distribution as calculated by the differential method using 29 meshes in the axial direction and 19 in the radial direction is indicated by the crosses. In addition the axial field  $B_{\text{coil}}$  due to the coil has been calculated by the Biot-Savart law. If this is subtracted from the total field distribution the result will be the magnetic field  $B_{\text{Fe}}$  produced along the axis by the iron circuit. The calculated field from the coil is exact and not affected by the position of the artificial boundary  $A=0$ . If now the field due to the iron, smoothed if necessary, is added to that of the field from the coil, an improved total field will result with only a trivial additional computing effort. The differential-integral method thus overcomes many of the weaknesses of the pure differential method. It is especially useful at the initial design stage where rapid interactive computing is essential.

#### Rotation-Free Projector Lenses

Compact windings with efficient water cooling<sup>14</sup> not only reduce considerably the size and weight of the electron optical column but it enables lenses to be grouped in pairs with the exciting coils wound in opposite directions, exactly compensating image rotation at all currents<sup>9</sup>. Fig. 11 shows the focal properties of a pair of projector lenses of conventional design but miniaturised in construction. The two lens gaps are separated by a distance of 50 mm. The focal properties of such a pair can be readily simulated by the square top magnetic field model.

The images at the top of the figure show typical images formed by this doublet. At low magnification (A) a distortion free picture of the grid is easily obtained. At very high magnification (D) essentially distortion free magnification is obtained. The lens system in this region has the same aberrations as that of the final projector lens acting on its own; a range of magnification of roughly three times can therefore be obtained with adequately low distortion. At the lower end of this range of magnification (Fig. B) characteristic pin-cushion distortion makes its appearance.

#### Single-Polepiece Projector Lenses

Single-polepiece lenses can have very favourable electron-optical and constructional properties. A very simple construction for a rotation-free single polepiece projector doublet is shown in Fig. 12. Here the lens body is machined from a single piece of iron. Coils are inserted in each of the lens units and the end faces sealed off with a non-ferromagnetic lid. The bore can be made quite large so that a vacuum liner tube can be used as shown in Fig. 13 which shows two such units installed in an experimental electron microscope. The upper lens unit serves as a rotation-free diffraction lens while the lower one serves as the rotation-free main projector. Fig. 14 shows a typical selected area diffraction pattern taken by a double exposure in which the diffraction lens operates as a weak lens to acquire the diffraction pattern and as a strong lens to acquire the resulting image of the molybdenum trioxide crystal. In conventional lens systems selected area diffraction patterns are subject to severe disorientation between the image and the corresponding diffraction pattern. A rotation-free projector system automatically preserves the correct orientation and incidentally eliminates chromatic aberration of rotation from the image.

#### Distortion-Free Wide-Angle Projector Systems

For the past fifty years, conventional projector lenses have been restricted by spiral distortion to a semi-angle  $\alpha_p$  of projection of about some  $5^\circ$ . This leads to excessively long viewing chambers (500-1000 mm) in TEM and difficulties of interfacing energy loss spectrometers in STEM. A wide-angle ( $\alpha = 30^\circ$ ) system would go a long way to solving these problems, and single polepiece lenses are uniquely suited to this purpose. The simple type of rotation-free doublet described above is not, however, optimised for this purpose. The reason for this is that the aberrations of a single-polepiece lens are lowest when the polepiece faces the incoming beam and largest when it faces away from the direction of the incident beam. In a correcting system the polepiece of the final projector lens must therefore face the incoming electron beam in order to produce minimum aberration at the fluorescent screen. The corrector lens on the other hand must face away from the direction of the electron beam in order to produce as much radial and spiral distortion as possible so that even after a magnification of 3x by this lens sufficient distortion will still be available to cancel that of the final projector lens. An early experimental scheme for producing a wide-angle

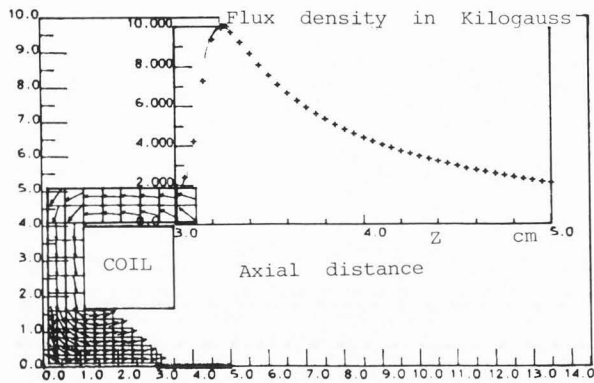


Fig. 9. Expanded detail from Fig. 8 with extra calculated points in the polepiece region giving improved accuracy.

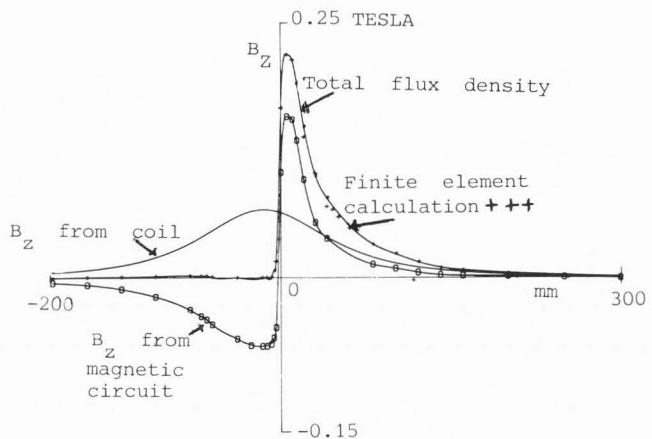


Fig. 10. Differential-Integral method (Mulvey and Nasr 1981) for improving the accuracy of the differential finite element method (Munro 1971). +++ calculated values from Munro program, —  $B_z$  due to coil, eeeeeee  $B_z$  due to iron, ●●●●● total  $B_z$ .

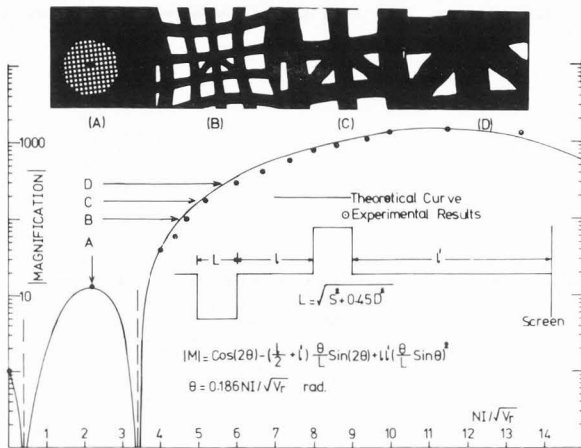


Fig. 11. Electron-optical characteristics of rotation-free projector doublet comprising two mini-lenses with conventional polepieces. Magnification can be calculated from square top model as indicated. Top magnification  $1200 \times$  for  $l' = 450$  mm. Micrographs A, B, C, D show distortion characteristics at different magnifications. Juma and Mulvey (1978)<sup>9</sup>.

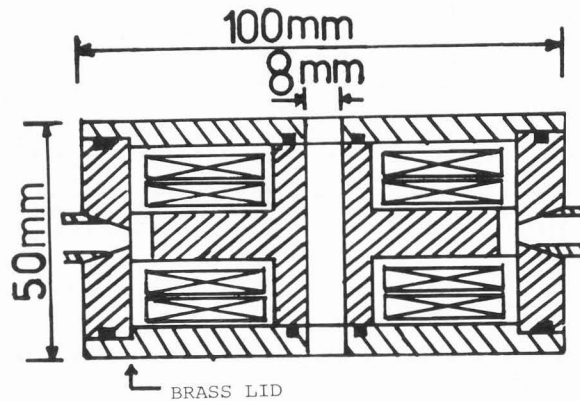
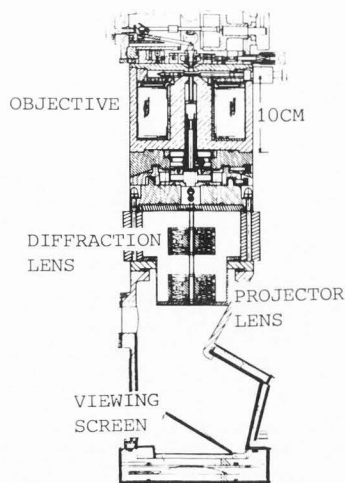


Fig. 12. Rotation-free miniature single-pole projector lens doublet for 100 kV electron microscope. Note the wide bore (8 mm) for vacuum liner. Juma and Mulvey (1978)<sup>9</sup>.

13



single polepiece lens doublet<sup>11</sup> is shown in Fig. 15. Here the electron beam passes through a corrector lens in the form of the lens of Fig. 12 but in which only the lower coil is energised. The beam then passes through a specially designed single-polepiece lens of low aberration provided with a conical exit in the lower polepiece to allow the passage of the beam of some  $30^\circ$  semi-angle. This experiment demonstrated the feasibility of making a wide-angle projector lens. It also confirmed calculations that the corrector lens needs about twice the excitation required by the projector lens resulting in considerable field cancellation by the two single polepieces of opposite polarities. This problem was overcome<sup>7</sup>

Fig. 13. Miniature rotation-free single-polepiece doublets as diffraction lens and final projector lens in a 100 kV electron microscope with vacuum liner tube fitted. Mulvey and Juma (1978)<sup>9</sup>.



in the design shown in Fig. 16 in which the corrector lens is physically larger than the final projector lens; a magnetic screen was also introduced between the two polepieces. The magnetic screen must be kept as far as possible from the projector lens polepiece in order to maintain the favourable field distribution for minimum spiral and radial distortion. The corrector lens must produce approximately ten times more distortion than that of the final projector, but of opposite sign, assuming that a corrector lens magnification of approximately 3.3 is required. The remarkable improvement in distortion-free operation is shown in Fig. 17. On the right is shown the calculated distortion pattern of the final projector alone with a semi-angle of  $30^\circ$ . Considerable spiral distortion is noticeable. The inner circle shows the virtually distortion-free pattern that is obtained in such a lens at a semi-angle of  $5^\circ$  as with a conventional projector lens. The left hand image is an image of a rectangular grid taken in an experimental electron microscope fitted with a wide-angle projector lens operating with a semi-angle of  $30^\circ$ . The final adjustment of this lens had to be carried out by trial and error methods since the marginal rays differed significantly from those calculated from the paraxial ray equation. Similarly, the presence of higher order aberrations made the image differ markedly from the predictions of third order aberration theory. It was therefore decided in a subsequent investigation to use the methods of computer-aided design assisted by the general ray equation<sup>1</sup> so that the real electron trajectories could be plotted directly without the need for third or higher order aberration theory.

Guided by the experience gained with the correcting system shown in Fig. 16, the projector lens doublet shown in Fig. 18 was designed and constructed. It is of integral construction and is shown mounted, for testing, inside the viewing chamber of a JEOL electron microscope type JEM50 between the existing final projector and the fluorescent screen giving the possibility of forming a wide-angle image of  $30^\circ$  semi-angle on a transmission fluorescent screen. It is an integral construction machined from a solid block of soft iron. Each end face carries a single polepiece and is also machined from a solid piece of iron. The single polepiece of the corrector lens is separated from the intermediate magnetic screen by a non-ferromagnetic spacer, and is essentially a very asymmetric double-pole lens designed to produce some 100% of spiral distortion, permitting a magnification of some 3.3 times while still being able to correct 10% of spiral distortion in the final image. The right-hand end plate contains a carefully designed single polepiece of exceptionally low spiral distortion; the polepiece is shaped to permit a wide-angle beam to traverse the lens freely. The field distribution of this lens is essentially that of the spherical field<sup>4</sup> model which has the lowest known spiral and radial distortion coefficient of any lens. The calculated field distribution through this lens and the corresponding paraxial trajectory for a ray of height 1 mm are shown in Fig. 19. Such a ray would leave the projector at a semi-angle of  $28^\circ$  as shown. These



Fig. 14. Electron micrograph of molybdenum crystal with selected area diffraction pattern in the correct orientation by the use of rotation-free single-polepiece diffraction lens system.

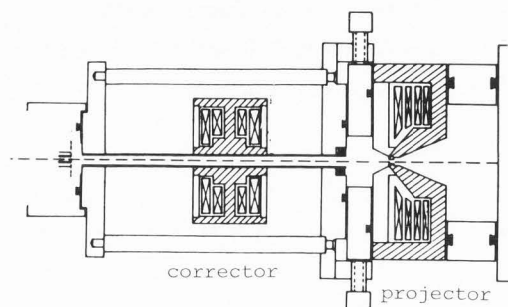


Fig. 15. Early experimental arrangement with two single-polepiece lenses for correcting spiral distortion in a wide-angle projector lens. Transmission fluorescent screen. Intermediate lens, mounted outside the vacuum, slides on vacuum liner for the cancellation of spiral distortion. Lambrakis et al (1977)<sup>11</sup>.

trajectories show that, at least to a first approximation, the shaping of the final polepiece was just sufficient to allow passage of the electron beam. This is an important point because the presence of too large a bore in a single polepiece lens degrades the desired field distribution and increases the spiral distortion coefficient. Calculation of the spiral and radial distortion coefficients for this lens on the basis of third order aberrations are shown in Fig. 20. Here a normalised distortion coefficient of radial distortion (solid line) and the corresponding quantity for spiral distortion (dotted line) are plotted against the excitation parameter  $NI/V_r^{3/2}$  of the corrector lens. This indicates that at an excitation parameter  $NI/V_r^{3/2}$  of 18 the radial and spiral distortion vanish simultaneously.

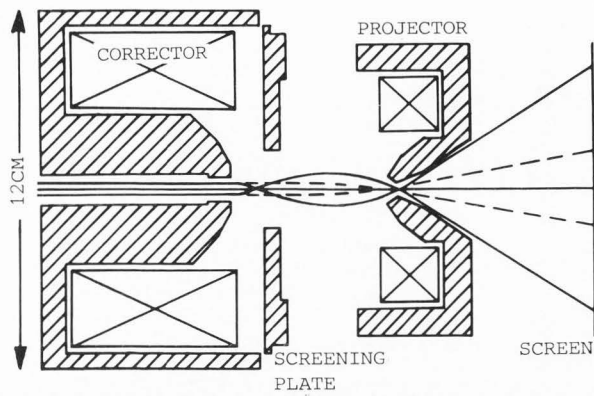


Fig. 16. Improved design of wide-angle projector lens. Semi-angle  $\alpha_p = 30^\circ$ . Full lines: paraxial ray calculation for parallel rays entering the corrector lens. Dashed lines: trajectories of same paraxial rays entering the system with the corrector lens de-energized. Note adjustable magnetic screen plate for avoiding field cancellation effects<sup>7</sup>.

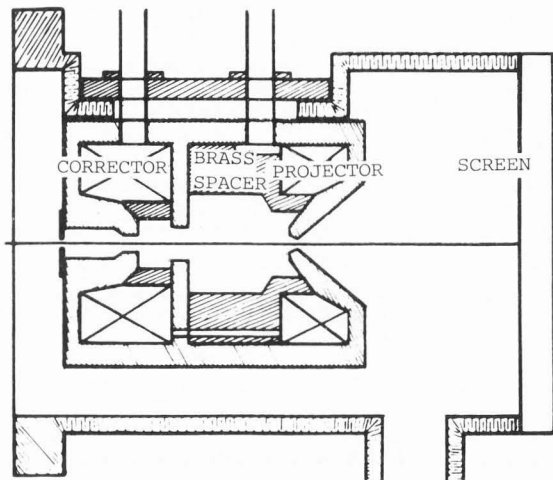


Fig. 18. Wide-angle projector lens unit<sup>1</sup> of integral construction mounted inside the viewing chamber of a JEOL JEM50 electron microscope. Semi-projection angle  $\alpha_p = 30^\circ$ .

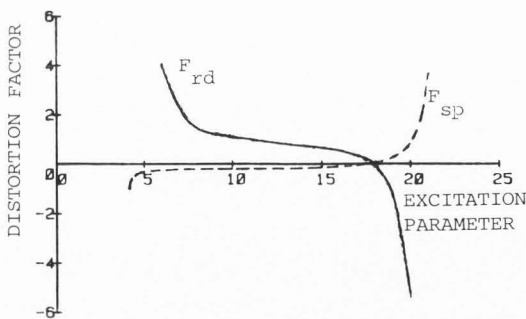


Fig. 20. Calculated radial distortion factor (solid line) and spiral distortion factor (dashed line) for the integral wide-angle projector unit as a function of the excitation parameter  $NI/V_r^2$  of the corrector lens.

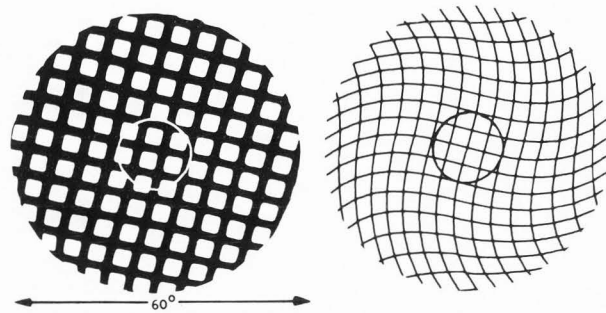


Fig. 17. Left. Experimentally obtained distortion-free image of a rectangular grid in a 100 kV electron microscope. Total angular field  $60^\circ$ . Inner circle indicates distortion-free field of view of a conventional projector lens. Right. Calculated distortion pattern of the projector lens acting alone over a total field of  $60^\circ$ . Micrograph by H El-Kamali.

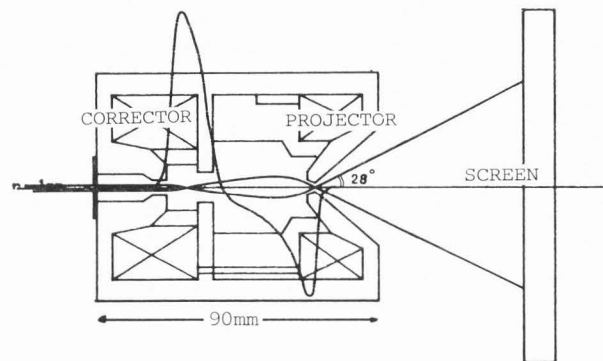


Fig. 19. Calculated axial field distribution and trajectories, calculated by the paraxial ray equation for an incoming ray of height 1 mm. Exit angle  $\alpha_p = 28^\circ$ .

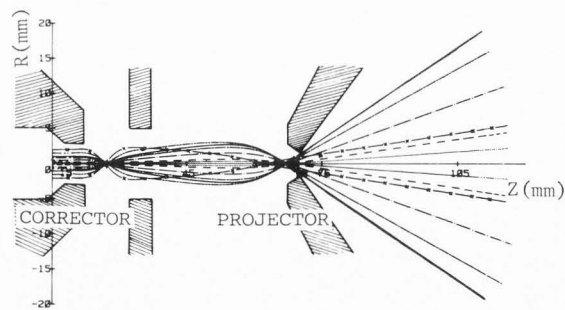


Fig. 21. Actual electron trajectories through the wide-angle projector system as calculated from the general ray equation. Trajectories indicate distortion-free operation up to a semi-angle  $\alpha_p = 30^\circ$ .

Moreover, the correction of the spiral distortion is not critical and remains at a fairly low value right up to the point of correction. This is a very useful property of this design since the correction point can be readily found experimentally by concentrating on the radial distortion in the image. However, this is a case in electron optical instrumentation in which the third order aberration theory can only be regarded as a rough guide. This was borne out by the experimental behaviour of the lens, which was broadly in line with the calculated values but there were important differences especially concerning the behaviour of the marginal rays. These took the form of an unwanted and highly distorted image inconveniently superimposed on an otherwise perfectly corrected image on the final screen. An explanation for this phenomenon was found when the real trajectories were plotted through the system from the general ray equation as shown in Fig. 21. Parallel rays entering the corrector lens are brought to a focus at the centre of the corrector lens and enter the field of the projector lens as a nearly parallel bundle of rays, as indicated by the (dotted) paraxial rays, forming an image at the centre of the fluorescent screen. This indicates that the corrector lens in this mode is forming a virtual image located to the left of the corrector lens. This means that the projector lens is effectively accepting a beam of approximately parallel incident electrons thereby reducing its own coefficients to a minimum. The exit angle of the ray is proportional to the radial height in the corrector lens up to the maximum semi-angle of the exit cone, as indicated by the solid line which just touches the inner edge of the polepiece of the projector lens. However, the bore of the corrector lens as designed will admit rays of even larger radius. For such rays, however, such as the one marked with a cross the aberrations of the corrector lens suddenly become excessively large and deliver a converging beam which strikes the principal plane of the projector lens and so is hardly refracted. This is the cause of the unwanted image originally seen at the centre of the fluorescent screen. The cure is simply to restrict the extreme marginal rays by an aperture of some 2 mm in diameter placed in the bore of the corrector lens. It can also be seen from Fig. 21 that the shaping of the projector polepiece in terms of paraxial rays has not been fully optimised for the real rays and minor changes in its shape could produce some further small improvements. The effectiveness of this corrector unit was in every way comparable with that of the previous experimental corrector unit shown in Figure 16, and images of the same quality as that of Figure 17 were obtained but without the need for any mechanical adjustment of the lens system. It also confirmed the view that an exit semi-angle  $\alpha_p = 30^\circ$  is probably the upper limit for a corrector device of this type. If such a lens were used in a conventional electron microscope with the normal viewing distance of some 450 mm, distortion-free operation of this type would be possible on a screen roughly half a metre in diameter. This investigation has shown that the use of the general ray equation can be very useful in the design of real electron optical

systems since it can often explain the apparently unusual behaviour of the electron optical system compared with the design expectations based on paraxial ray theory.

#### Scanning Transmission Electron Microscopes with Advanced Electron-Optical Systems

The STEM was invented in 1938 by von Ardenne but lay in abeyance until the late 1960s when Crewe and his colleagues introduced an experimental STEM with a field emission electron gun. In its original form, Crewe's system was very simple consisting of a field emission gun, a condenser lens and a final probe forming lens. Interestingly Crewe chose the Riecke/Ruska condenser-objective lens as a final probe forming lens. The first part of this lens (the condenser part) was used in conjunction with the preceding condenser lens to focus the incoming beam on the specimen; the second (objective) part was used to converge the scattered beam from the specimen conveniently into the electron detector. Such an instrument is particularly well suited to high resolution dark field microscopy and is capable of the same resolution as a TEM with an objective lens of the same spherical aberration coefficient at the same accelerating voltage. The output from a STEM is automatically in a form that is suitable for direct interfacing to a computer for subsequent image processing. It is also possible to allow the inelastically scattered electrons to pass into an electron velocity spectrometer whose output can also be displayed as an image on the display tube. So far, the accelerating voltage of STEM instruments has been restricted to 50-100 kV and so it has not yet been possible to compare STEM and TEM at very high resolution.

#### Analytical STEMS

In the meantime attention has been turning more to improving the STEM as a micro-analytical tool for the quantitative examination of micro-regions in thin specimens. Operators of analytical TEMs are accustomed to being able to obtain, in addition to the image, both conventional and convergent beam diffraction patterns from selected micro-regions. One might also wish to obtain characteristic x-ray spectra by means of an energy dispersive detector or an electron energy loss spectrometer. In the latter case it is desirable to match the angular spread of the electrons leaving the specimen to that of the electron beam that can enter the spectrometer. This can only be done by adding a number of post-specimen projector lenses. At the same time it is advantageous to have a means of converting the scanned electron beam leaving the specimen into a static beam falling on to the various fixed detectors which can then include a fluorescent screen for recording diffraction patterns. The latter is almost essential since the normal serial method of acquiring a diffraction pattern in a STEM is extremely time-consuming. Fig. 22 shows an experimental analytical STEM of this type<sup>6</sup> designed by Professor Ferrier and his team at Glasgow University. A standard Vacuum Generator's field emission gun STEM forms the basis of the instrument. The lower, probe-forming, part of the column consists of the field emission gun, two condenser lenses and a Riecke/Ruska lens as a final probe-forming lens. Two condenser lenses are used to enable greater freedom in operating

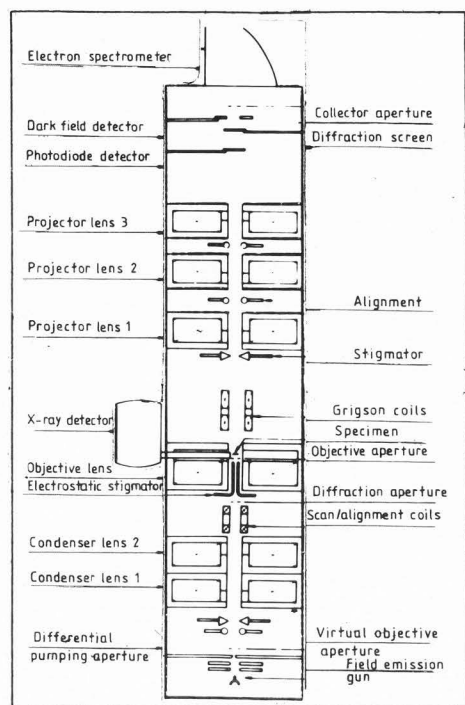


Fig. 22. Schematic arrangement of an analytical STEM<sup>6</sup> at Glasgow University. Note the projector lens system for providing a static diffraction pattern and an interface between the specimen and the energy loss spectrometer.

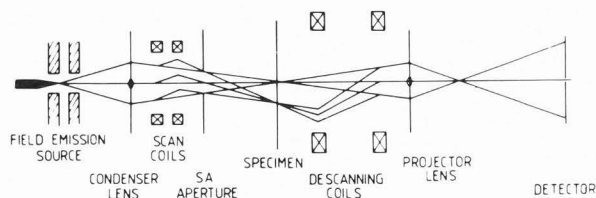


Fig. 23. Schematic arrangement of the complete ray path in the analytical STEM<sup>6</sup> showing the action of the scanning coils and the "de-scanning" coils for producing a static image.

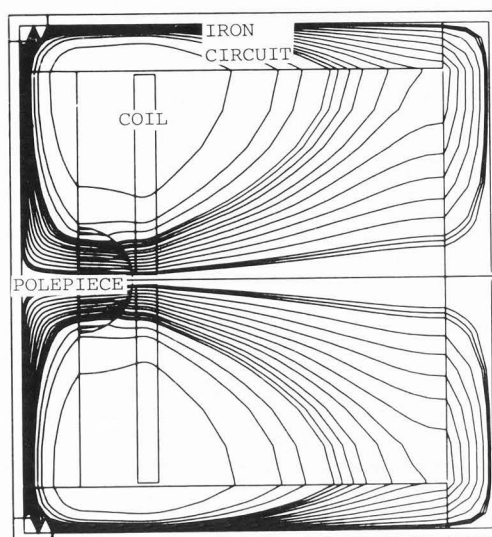


Fig. 24. Flux distribution in a single-polepiece lens with a spherical pole-tip energized by an optimised coil design<sup>3</sup>. Peak flux density on the axis 3.4 Tesla. Outside diameter 72 mm. Excitation 30 kA-t.

the latter lens. The x-ray detector is an energy dispersive (EDX) system that allows a characteristic x-ray spectrum to be obtained from a chosen point on the specimen. Above the specimen are the normal diffraction scan coils which can also be used to "de-scan" the electron beam leaving the specimen as indicated in Fig. 23 which shows schematically the complete ray path of the beam from source to detector. The "de-scan" removes the scanning motion of the electron beam leaving the sample so that a steady image of a diffraction pattern may be viewed on a fluorescent screen or recorded on a photo-diode detector. The three post-specimen projector lenses between the specimen and the fluorescent screen enable the magnification of the various images to be adjusted. Similarly the angular aperture of the beam entering the spectrometer can be optimised to that leaving the specimen. All the problems previously mentioned in connection with wide-angle projectors are relevant here. In addition there is the extra requirement that the lens units must be fully compatible with high vacuum procedures such as "bakeout". To control an instrument of this type manually would be extremely time-consuming and so computer control has become essential both in adjusting the instrument and in data handling.

#### Future Developments in Magnetic Electron Lenses and Lens Systems

The future development of high resolution magnetic electron lenses must lie in the greater

attention to detail in the design of the exciting coil in order to achieve higher flux densities. In a conventional lens the exciting coil makes a negligible contribution to the axial field distribution, nearly all of which is produced by the magnetisation of the iron polepieces. As the lens excitation is increased these polepieces and often other parts of the magnetic circuit begin to saturate. Further increase of lens excitation leads to a broadening of the field distribution, and an effective limitation to the maximum flux density that can be achieved. Many of these effects can be reduced by the optimum placing of the coil<sup>2</sup>. Figure 24, for example, shows a single polepiece lens with a spherical tip in which a thin coil of high ratio of outer to inner diameter is placed in close proximity to the tip<sup>3</sup>. The resulting field distributions are shown in Figure 25. It can be seen that even at high peak axial flux densities approaching 4 Tesla the field broadening is remarkably small. The reason for this is that in this particular design the saturation magnetization of the iron is strongly localised at the tip. Hence in the vicinity of the polepiece the saturation flux density is

simply added to the field produced by the coil. In this type of lens, therefore, there is no limit to the maximum flux density that can be produced except that set by the maximum permissible current density in the exciting coil. With super-conducting windings, for example, this permissible current density is of the order of  $10^{10}$  A/m<sup>2</sup>. These lenses, therefore, are not limited so much by the properties of the iron but largely by the technology of super-conducting windings. Similar principles can be applied to the double polepiece lens of the condenser-objective type as shown in Fig. 26, which shows the flux distribution in a twin-polepiece lens with a central coil of high ratio of outside to inside diameter. Here again high fluxes can be produced at the specimen position in the centre of the lens as shown in Fig. 27 which also shows the magnetization component of the axial flux density distribution created by the iron. Fig. 28 shows the axial flux density distribution in this lens for a vanishingly small polepiece bore. These results suggest that an increase in maximum flux density up to 4 Tesla is feasible for high resolution objective lenses. However, it should be mentioned that, for a given accelerating voltage, the excitation of such a lens is a fixed quantity. Thus the only way to achieve a higher flux density in an objective lens of optimised shape is to reduce its size. This is largely a question of superconductor technology. For complete electron-optical columns, intermediate lenses can conveniently be rotation-free lenses of miniature construction and modest flux density. These can often be conveniently accommodated within the internal bores of conventional lenses as described for example by Podbrdsky<sup>16</sup>. The alignment of such lenses and the setting of the excitation can readily be controlled by a mini-computer. Such systems will provide and record a vast amount of quantitative data from the specimen and will be physically more compact than present designs. In addition they will lend themselves to automatic or semi-automatic operation under computer-control.

#### Acknowledgements

The author would like to place on record the considerable contribution of a long line of postgraduate researchers who have contributed ideas, experiments and theory to the investigations reported in this paper and whose original work is cited in the text and in the references. These include Drs Christopher Newman, Richard Bassett, Fathi Marai, Emmanuel Lambrakis, Sabah Juma, Peter Harris, Stelios Christofides, Adil Al Shwaikh, Hisham El-Kamali, Hamid Nasr, Shatha Al-Hilly, Muna Al Khashab and In'am Al-Nakeshli. He would also like to thank Professor Armin Delong, Dr Josef Podbrdský, Dr Jiří Komrská, Dr Bohumila Lencová and Dr Michael Lenc of the Institute of Scientific Instruments at Brno, Czechoslovakia for stimulating discussions on the practical realisation of completely new forms of electron optical columns. He is also indebted to Dr Eric Munro, of Imperial College, London, and Mr C W Trowbridge of the Rutherford-Appleton Laboratory, Didcot, UK, for valuable discussions

on the mathematical basis of the finite element method. He would also like to thank Mr Wenxiong Cheng of Beijing University for his contribution to computing methods in electron optics during his sabbatical year at Aston University. This list would not be complete without mentioning the skilful workmanship and technical know-how of Messrs Howard Arrowsmith, Ken Bates, Roland Keen and Frank Lane of the Physics Workshop in the practical realisation of new forms of magnetic electron lenses.

#### References

1. Al-Hilly SM, Mulvey T. (1981). Wide-angle projector systems for the TEM. *Inst. Phys. Conf. Series No. 61*, M J Goringe (ed), 103-106.
2. Al Khashab M. (1983). The electron optical limits of performance of single polepiece magnetic electron lenses. PhD dissertation, University of Aston in Birmingham.
3. Al-Nakeshli IS, Juma SM, Mulvey T. (1983). High flux density single polepiece electron lenses. *Inst. Phys. Conf. Series No. 68*, 475-478.
4. Alshwaikh A, Mulvey T. (1977). The magnetised iron sphere, a realistic theoretical model for single-polepiece lenses. *Inst. Phys. Conf. Series No. 36*, 25-28.
5. Busch H. (1927). On the mode of action of the concentrating coil in the Braun tube. *Arch. Elektrotech.* 18, 583-594.
6. Chapman JN, Morrison GR, Ferrier RP. (1980). *Proc. 7th Eur. Conf. Elec. Micros. The Hague* 1, 90-91. *7th Eur. Conf. Foundation. Leiden, 1980.*
7. El Kamali H, Mulvey T. (1980). A wide-angle TEM projection system. *Proc. 7th Eur. Conf. Elec. Micros. The Hague* 1, 74-75. *7th Eur. Conf. Foundation. Leiden, 1980.*
8. Gabor D. (1926). Doctoral Dissertation, Technological University of Berlin. Oscillographic recording of travelling waves with the cathode ray oscillograph. In German.
9. Juma SM, Mulvey T. (1978). Rotation-free magnetic electron lenses. *J. Phys. E.* 11, 759-764.
10. Knoll M, Ruska E. (1931). Contribution to geometrical electron optics. *Ann. Phys.* 12, 607-640.
11. Lambrakis E, Marai FZ, Mulvey T. (1977). Correction of spiral distortion in the TEM. *Inst. Phys. Conf. Series No. 36*, 35-38.
12. Lencová B, Lenc M. (1984). The computation of open electron lenses by coupled finite element and boundary integral methods. *Optik* (in press).
13. Mulvey T, Nasr H. (1981). An improved finite element method for calculating the magnetic field distribution in magnetic electron lenses and electromagnets. *Nucl. Instr. Meth.* 187, 201-208.
14. Mulvey T. (1982). Chapter 5 in *Magnetic Electron Lenses*, ed. PW Hawkes, Springer-Heidelberg, 351-412.

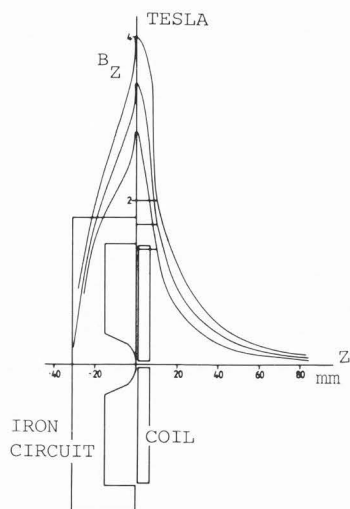


Fig. 25. Axial flux density distributions as a function of excitation for optimised single-polepiece lens<sup>3</sup>, for excitations of 40, 60, and 80 kA-t. Peak axial flux 4 Tesla with relatively small broadening.

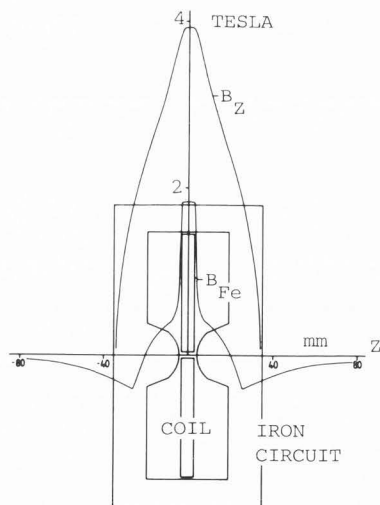


Fig. 27. Axial flux density distribution  $B_z$  in the air gap and the iron circuit of twin polepieces without a bore<sup>3</sup>.  $B_{Fe}$  is the axial flux density distribution contributed by the iron for a polepiece having a vanishingly small bore<sup>3</sup>.

15. Munro E. (1981). PhD Dissertation. Computer design methods in electron optics, University of Cambridge, UK.

16. Podbrdský J. (1980). The optical system of the analytical electron microscope with mini-lenses. Proc. 7th Eur. Conf. Elec. Micros. The Hague 1, 66-67. 7th Eur. Conf. Foundation. Leiden, 1980.

17. Riecke WD, Ruska E. (1966). A 100 kV TEM with single field condenser-objective lens. Proc. Int. Conf. Kyoto 1, 19-20. Maruzen. Tokyo, 1966.

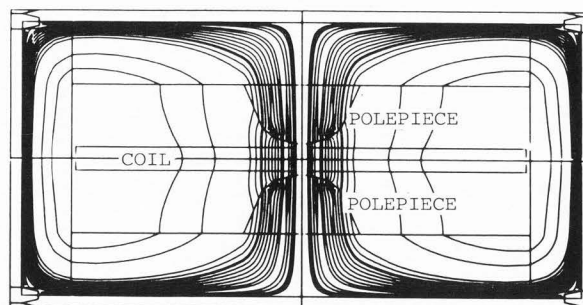


Fig. 26. Flux distribution in twin-polepiece lens with optimised exciting coil<sup>3</sup>. Peak axial flux density 4 Tesla.

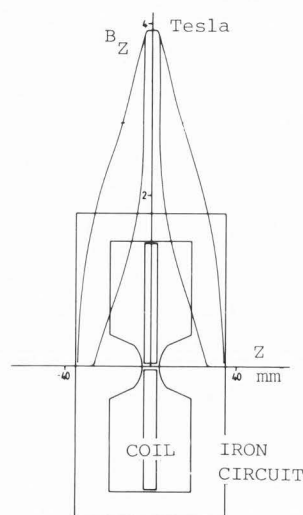


Fig. 28. Axial flux density distribution in a double polepiece lens<sup>3</sup> of vanishingly small bore. Lens excitation 60 kA-t. Soft iron polepieces.

18. Smith KCA, Swann DJ. (1969). UK Patent 1291221.

19. Trowbridge CW. (1976). Applications of integral equation methods for the numerical solution of magnetostatic and eddy current problems. Int. Conf. Elec. and Mag. field problems Santa Margherita, Italy, 1-22. (Available from Rutherford Laboratory, Didcot, OX11 0QX (UK).)

20. Troyon M, Laberrigue A. (1977). A field emission gun with high beam current stability. J. Microsc. Spectrosc. Electron. 2, 7-11.

21. Venables JA, Archer GD. (1980). On the design of FEG-SEM columns. Proc. 7th Eur. Conf. Elec. Micros. The Hague 1, 54-55. 7th Eur. Conf. Foundation. Leiden, 1980.

22. Von Borries B, Ruska E. (1932). German Patent No. 680284. Magnetic converging lens of short focal length.